



# CHORUS

This is the accepted manuscript made available via CHORUS. The article has been published as:

## Increasing photocell power by quantum coherence induced by external source

Konstantin E. Dorfman, Moochan B. Kim, and Anatoly A. Svidzinsky

Phys. Rev. A **84**, 053829 — Published 14 November 2011

DOI: [10.1103/PhysRevA.84.053829](https://doi.org/10.1103/PhysRevA.84.053829)

# Increasing photocell power by quantum coherence induced by external source

Konstantin E. Dorfman,\* Moochan B. Kim, and Anatoly A. Svidzinsky  
Texas A&M University, College Station, TX 77843

We show that photocell power can be substantially enhanced by quantum coherence in the model proposed by M.O. Scully, Phys. Rev. Lett. 104, 207701 (2010). Here coherence is induced by an external microwave drive. We show that although such coherence requires an extra energy input the amount of extra input power can be much smaller than produced enhancement of the photovoltaic power. We demonstrate that for certain parameters power enhancement is governed by quantum coherence and not just a result of population transfer due to the driving field.

PACS numbers:

## I. INTRODUCTION

Quantum coherence yields interesting effects in laser physics, chemical physics and optics. Examples include lasing without population inversion [1, 2], electromagnetically induced transparency [3], slow light [4] in atomic systems, semiconductor quantum dots [5] and heterostructures [6]. Furthermore it has been shown that heat engines can benefit from quantum coherence by extracting more useful work from a single thermal reservoir [7]. Heat engine is an important example. For instance, in 1954 Scovil and Schulz-DuBois [8] demonstrated that maser (laser) is a quantum heat engine that transforms energy of the hot thermal photons into low entropy coherent radiation. Moreover, Schockley and Queisser [9] obtained their famous “detailed balance” limit by studying the photovoltaic cell illuminated by “hot” thermal light that deliver useful work to the load. However quantum coherence can break the detailed balance relation between absorption and emission as, e.g., in lasing without inversion [2, 10].

In the seminal article [11] quantum coherence induced by an additional driving field was integrated into a photovoltaic system. It was shown that this can increase the open circuit voltage of the quantum dot photocell (see Fig. 1). The coherence in [11] was generated by external microwave field resonantly driving  $1 \leftrightarrow 2$  transition. However the actual power delivered to the load by the photocell was not calculated. In recent papers [12, 13] another mechanism of coherence generation was studied that does not require an external source. It was found that noise induced coherence via Fano interference [14] can enhance the balance breaking [15] and increase the photocell power delivered to the load or power of quantum heat engines, such as lasers [16, 17].

The “toy model” of Ref. [11] with coherence induced by an external drive raised issues that need to be addressed. For instance, what is the role of coherence in the model with external drive? Is the improvement of performance caused by the drive itself or by coherence? What is the power of microwave source that is required to produce such an enhancement?

In the present paper we investigate those questions and show in details that the photocell model with coherence induced by driving field can yield substantial enhancement of

the photocell power even if the power of the drive is insignificant. We also show that generated coherence can be robust against environmental  $\tau_2$  effects.

## II. THREE-LEVEL MODEL WITH COHERENTLY DRIVEN UPPER DOUBLET

As an introduction, we first consider equations for a simple three-level model. Namely, we have in mind a single quantum dot with two upper levels  $|1\rangle$  and  $|2\rangle$  resonantly driven by a microwave field. At the same time both  $|1\rangle$  and  $|2\rangle$  states decay to the same ground state  $|b\rangle$ .

The interaction Hamiltonian in the rotating-wave approximation consists of two parts

$$\hat{V}(t) = \hat{V}_\mu(t) + \hat{V}_{th}(t), \quad (1)$$

where interaction between microwave field and quantum dot is described by

$$\hat{V}_\mu(t) = -\hbar\Omega [e^{-i\phi}|1\rangle\langle 2| + h.c.]. \quad (2)$$

Here microwave field is characterized by Rabi frequency  $\Omega = \mathcal{P}_{12}\mathcal{E}/2\hbar$  and phase  $\phi$ , where  $\mathcal{E}$  is the electric field and  $\mathcal{P}_{12}$  is the dipole matrix element of the  $1 \leftrightarrow 2$  transition. Interaction between electrons and thermal radiation field is given by

$$\hat{V}_{th}(t) = \hbar \sum_{\mathbf{k}} \left[ g_{1\mathbf{k}}|1\rangle\langle b|\hat{a}_{\mathbf{k}}e^{i(\omega_1-\nu_{\mathbf{k}})t} + g_{2\mathbf{k}}|2\rangle\langle b|\hat{a}_{\mathbf{k}}e^{i(\omega_2-\nu_{\mathbf{k}})t} + h.c. \right], \quad (3)$$

where  $\hat{a}_{\mathbf{k}}$  is the field operator,  $\nu_{\mathbf{k}}$  are frequencies of the radiation field,  $\omega_j$  ( $j = 1, 2$ ) are the corresponding electronic transition frequencies. We assume that narrow band thermal radiation is peaked around  $\omega_j$  and pump both levels  $|1\rangle$  and  $|2\rangle$ . The radiation thermal reservoir is described by the density operator  $\hat{\rho}_R$ . Taking into account that  $\langle \hat{a}_{\mathbf{k}} \rangle = \langle \hat{a}_{\mathbf{k}}^\dagger \rangle = 0$  for thermal field the equation of motion for the electronic density operator  $\hat{\rho}$  reads [2]

$$\begin{aligned} \dot{\hat{\rho}}(t) = & -\frac{i}{\hbar}\text{Tr}_R \left[ \hat{V}_\mu(t), \hat{\rho}(t) \otimes \hat{\rho}_R(t_0) \right] \\ & - \frac{1}{\hbar^2}\text{Tr}_R \int_{t_0}^t \left[ \hat{V}_{th}(t), \left[ \hat{V}_{th}(t'), \hat{\rho}(t') \otimes \hat{\rho}_R(t_0) \right] \right] dt'. \quad (4) \end{aligned}$$

\* Corresponding author, email: dorfmank@gmail.com

We assume that levels  $|1\rangle$  and  $|2\rangle$  are close to each other and in our model we do not include coupling between them apart from the driving field. Also we neglect possible interference due to interaction of electronic system with radiation and phonon thermal reservoir (such as noise induced coherence) and focus on the effect of the microwave drive.

Equations for the density matrix elements  $\rho_{ij} \equiv \langle i|\hat{\rho}|j\rangle$  in the Weisskopf-Wigner approximation read

$$\dot{\rho}_{11} = -\gamma_1[(n_1+1)\rho_{11} - n_1\rho_{bb}] + i\Omega[\rho_{21}e^{-i\phi} - \rho_{12}e^{i\phi}], \quad (5)$$

$$\dot{\rho}_{22} = -\gamma_2[(n_2+1)\rho_{22} - n_2\rho_{bb}] - i\Omega[\rho_{21}e^{-i\phi} - \rho_{12}e^{i\phi}], \quad (6)$$

$$\begin{aligned} \dot{\rho}_{12} = & -i\Omega e^{-i\phi}(\rho_{11} - \rho_{22}) - \frac{\rho_{12}}{\tau_2} \\ & - \frac{1}{2}[(\gamma_1(n_1+1) + \gamma_2(n_2+1))\rho_{12}], \end{aligned} \quad (7)$$

where  $\gamma_j$  ( $j = 1, 2$ ) are spontaneous decay rates and  $\tau_2$  is the decoherence time. Average photon numbers  $n_1$  and  $n_2$  driving the  $|1\rangle \leftrightarrow |b\rangle$  and  $|2\rangle \leftrightarrow |b\rangle$  transitions at solar temperature  $T_S$  are given by

$$n_{1,2} = \frac{1}{\exp\left(\frac{E_{1,2} - E_b}{k_B T_S}\right) - 1}. \quad (8)$$

### III. QUANTUM PHOTOCELL WITH COHERENT DRIVE

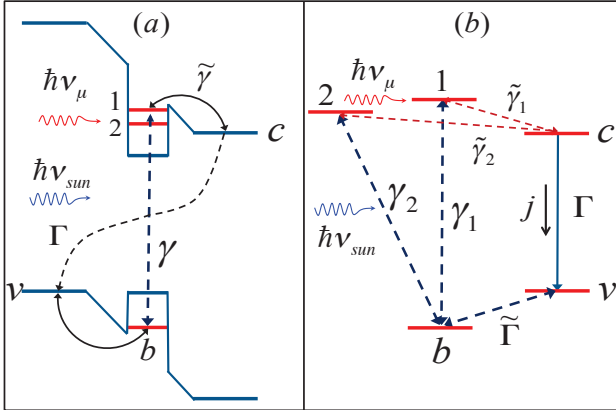


FIG. 1. (Color online) (a) Quantum dot photocell with lower level  $|b\rangle$  in the valence band and two upper levels  $|1\rangle$  and  $|2\rangle$  in the conduction band resonantly driven by a coherent field with energy  $\hbar\nu_\mu$  and Rabi frequency  $\Omega$  coupled to conduction  $|c\rangle$  and valence  $|v\rangle$  reservoir states. (b) Corresponding energy level diagram of the cell model. Solar radiation with energy  $\hbar\nu_{sun}$  drives transitions between the ground state  $|b\rangle$  and the two upper levels. Transitions  $|1, 2\rangle \leftrightarrow |c\rangle$  and  $|b\rangle \leftrightarrow |v\rangle$  are driven by ambient thermal phonons. Levels  $|c\rangle$  and  $|v\rangle$  are connected to a load.

Next we generalize our equations for the case of a photovoltaic cell shown in Fig. 1 which consists of a single quantum dot with two levels  $|1\rangle$  and  $|2\rangle$  in the conduction band

and level  $|b\rangle$  in the valence band. Levels  $|1\rangle$  and  $|2\rangle$  are coupled to the conduction reservoir state  $|c\rangle$ . State  $|b\rangle$  is coupled to the valence band reservoir state  $|v\rangle$ . Two upper levels are spaced by  $2\hbar\Delta$  and resonantly driven by the microwave field with Rabi frequency  $\Omega$ . The narrow band solar radiation at temperature  $T_S$  containing energies resonant to both transitions  $E_1 - E_b$  and  $E_2 - E_b$  is directed onto the cell and drives  $b \leftrightarrow 1, 2$  transitions with the average photon number given by Eq. (8). Ambient thermal phonons at temperature  $T_a$  couple the low energy transitions  $c \leftrightarrow 1, 2$  and  $b \leftrightarrow v$  and have occupation numbers

$$n_{c1,2} = \frac{1}{\exp\left(\frac{E_{1,2c}}{k_B T_a}\right) - 1} \quad \text{and} \quad n_v = \frac{1}{\exp\left(\frac{E_{vb}}{k_B T_a}\right) - 1}. \quad (9)$$

Moreover, we assume that levels  $c$  and  $v$  are connected to a load (e.g. resistor), and level  $v$  decays into the ground state  $b$  at a rate  $\tilde{\Gamma}$  (see Fig. 1b). We model the load by assuming level  $c$  decays into  $v$  at a rate  $\Gamma$ .

If level spacing between  $|1\rangle, |2\rangle$  and  $|c\rangle$  is small then coupling between those levels is due to acoustic phonons, while for large spacing it is governed by optical phonons. Starting from Eqs. (5) - (7) one can obtain equations of motion for the density matrix elements of the photocell model of Fig. 1. Introducing notation  $\rho_{12} = \tilde{\rho}_{12}e^{-i\phi}$  we find

$$\begin{aligned} \dot{\rho}_{11} = & -\gamma_1[(n_1+1)\rho_{11} - n_1\rho_{bb}] \\ & -\tilde{\gamma}_1[(n_{c1}+1)\rho_{11} - n_{c1}\rho_{cc}] + 2\Omega\text{Im}[\tilde{\rho}_{12}], \end{aligned} \quad (10)$$

$$\begin{aligned} \dot{\rho}_{22} = & -\gamma_2[(n_2+1)\rho_{22} - n_2\rho_{bb}] \\ & -\tilde{\gamma}_2[(n_{c2}+1)\rho_{22} - n_{c2}\rho_{cc}] - 2\Omega\text{Im}[\tilde{\rho}_{12}], \end{aligned} \quad (11)$$

$$\begin{aligned} \text{Im}[\dot{\tilde{\rho}}_{12}] = & -\Omega(\rho_{11} - \rho_{22}) - \frac{1}{\tau_2}\text{Im}[\tilde{\rho}_{12}] \\ & - \frac{1}{2}[(\gamma_1(n_1+1) + \gamma_2(n_2+1))\text{Im}[\tilde{\rho}_{12}]] \\ & - \frac{1}{2}[\tilde{\gamma}_1(n_{c1}+1) + \tilde{\gamma}_2(n_{c2}+1)]\text{Im}[\tilde{\rho}_{12}], \end{aligned} \quad (12)$$

$$\begin{aligned} \dot{\rho}_{cc} = & \tilde{\gamma}_1[(n_{c1}+1)\rho_{11} - n_{c1}\rho_{cc}] \\ & + \tilde{\gamma}_2[(n_{c2}+1)\rho_{22} - n_{c2}\rho_{cc}] - \Gamma\rho_{cc}, \end{aligned} \quad (13)$$

$$\dot{\rho}_{vv} = \Gamma\rho_{cc} - \tilde{\Gamma}(n_v+1)\rho_{vv} + \tilde{\Gamma}n_v\rho_{bb}, \quad (14)$$

$$\rho_{bb} + \rho_{11} + \rho_{22} + \rho_{cc} + \rho_{vv} = 1, \quad (15)$$

where  $\gamma_{1,2}$  and  $\tilde{\gamma}_{1,2}$  are spontaneous decay rates of the corresponding transitions (see Fig. 1b),  $\tau_2$  is the decoherence time. It is worth noting, that in the present model there is no explicit dependence on the phase of the microwave field  $\phi$ . However, there is dependence on the field amplitude governed by the Rabi frequency  $\Omega$ .

We focus on steady state operation. In this regime one can solve Eqs. (10) - (15) and obtain level populations and coherence  $\tilde{\rho}_{12}$ . For the moment we neglect decoherence  $\tau_2$  by setting  $1/\tau_2 \equiv 0$ . Interesting case arises when one of the phonon

decay rates, for example  $\tilde{\gamma}_2$ , is very small:  $\tilde{\gamma}_2 \ll \tilde{\gamma}_1, \gamma_1, \gamma_2$ . In this limit for  $\gamma_1 \approx \gamma_2 = \gamma, \Gamma \ll \tilde{\gamma}_1 n_c$  and  $n \ll n_c, n_v$  with  $n_{c,v} \gg 1$  the current through the cell  $j$  is given by

$$\frac{j}{e} \equiv \Gamma \rho_{cc} = \frac{\gamma \tilde{\gamma}_1 n_{c1} n_1 + 4(n_1 + n_2) \Omega^2}{2\gamma \tilde{\gamma}_1 n_{c1} + 8\Omega^2} \gamma, \quad (16)$$

while coherence is

$$\tilde{\rho}_{12} = \frac{i\gamma\Omega n_2}{\gamma \tilde{\gamma}_1 n_{c1} + 4\Omega^2}. \quad (17)$$

For weak microwave field  $\Omega^2 \ll \gamma \tilde{\gamma}_1 n_{c1}$  Eq. (16) yields

$$j \equiv j_0 = \frac{1}{2} e \gamma n_1, \quad (18)$$

while for strong drive  $\Omega^2 \gg \gamma \tilde{\gamma}_1 n_{c1}$  there is nearly 100% current enhancement

$$j \equiv j_\Omega = \frac{1}{2} e \gamma (n_1 + n_2). \quad (19)$$

In the present model voltage across the cell is expressed in terms of populations of the levels  $c$  and  $v$  connected to the load as

$$eV = E_c - E_v + k_B T_a \ln \left( \frac{\rho_{cc}}{\rho_{vv}} \right), \quad (20)$$

where  $T_a$  is the ambient temperature. Power delivered to the load is  $P = j \cdot V$ . The current-voltage characteristic of the cell can be obtained by varying the rate  $\Gamma$  at fixed other parameters.  $\Gamma = 0$  corresponds to the open circuit, while large  $\Gamma$  is the short circuit limit. Note that in our model, in addition to sunlight, there is microwave source pumping energy into the system. For the parameters discussed above the open circuit voltage is given by

$$eV_{oc} = E_1 - E_b + k_B T_a \log \left[ \frac{\gamma \tilde{\gamma}_1 n_1 n_{c1} + 4(n_1 + n_2) \Omega^2}{\gamma \tilde{\gamma}_1 n_{c1} + 8\Omega^2} \right]. \quad (21)$$

For weak driving field  $\Omega^2 \ll \gamma \tilde{\gamma}_1 n_{c1}$  Eq. (21) yields Carnot limit formula with energy source at temperature  $T_S$  and energy sink at temperature  $T_a$

$$eV_{oc} = (E_1 - E_b) \left( 1 - \frac{T_a}{T_S} \right). \quad (22)$$

However, for strong drive  $\Omega^2 \gg \gamma \tilde{\gamma}_1 n_{c1}$  we obtain

$$eV_{oc} = E_1 - E_b + k_B T_a \log \left[ \frac{n_1 + n_2}{2} \right]. \quad (23)$$

For small splitting of levels  $|1\rangle$  or  $|2\rangle$ ,  $\hbar\Delta \ll k_B T_S$ , taking into account Eq. (8), we find

$$eV_{oc} = (E_1 - E_b) \left( 1 - \frac{T_a}{T_S} \right) + \hbar\Delta \frac{T_a}{T_S}. \quad (24)$$

Note, that even in the case of strong drive the quantum efficiency (open circuit voltage) is always smaller than that

given by the Carnot limit since the input energy has an additional term due to microwave energy source that is  $E_{\text{input}} = E_1 - E_b + 2\hbar\Delta$ .

Next we estimate the energy input from external microwave source. According to Eqs. (10) and (11), the number of acquired microwave photons per second is given by

$$\frac{j_\mu}{e} = 2\Omega \text{Im}[\tilde{\rho}_{12}]. \quad (25)$$

Eqs. (16) and (17) yield that microwave current  $j_\mu$  can be expressed in terms of the photo-current  $j$  as

$$j_\mu = \frac{4\Omega^2 n_2}{\gamma \tilde{\gamma}_1 n_1 n_{c1} + 4(n_1 + n_2) \Omega^2} j. \quad (26)$$

For the weak drive,  $j_\mu \sim \Omega^2$ , while for a strong drive  $\Omega^2 \gg \gamma \tilde{\gamma}_1 n_{c1}$  taking into account Eq. (19) we find

$$j_\mu = \frac{1}{2} e \gamma n_2. \quad (27)$$

Thus, Eqs. (18), (19) and (27) show that photovoltaic current with strong drive  $j_\Omega$  is a sum of photocurrent with weak drive  $j_0$  and the current associated with the microwave field  $j_\mu$

$$j_\Omega = j_0 + j_\mu. \quad (28)$$

However, the power of microwave source that creates coherence is given by

$$P_\mu = j_\mu \cdot \frac{2\hbar\Delta}{e}, \quad (29)$$

while photocell power is  $P = j \cdot V$ , where the cell voltage  $V \gg \hbar\Delta/e$ . Therefore, substantial photocell power enhancement  $\delta P = j_\mu \cdot V$  can arise from quite small microwave input  $P_\mu = j_\mu \cdot 2\hbar\Delta/e \ll \delta P$ .

Next we calculate cell power and current by numerical solution of Eqs. (10)-(15) in steady state. Fig. 2 shows cell power as a function of voltage across the load for different values of  $\Omega = 0, 10\gamma, 25\gamma, 50\gamma, 100\gamma$  and  $500\gamma$ . In simulation we assume that levels  $|1\rangle$  and  $|2\rangle$  have energy spacing  $E_1 - E_2 = 0.2$  meV and take  $T_S = 0.5$  eV,  $T_a = 0.0259$  eV,  $E_1 - E_b = 0.7$  eV (typical band-gap for PbS or InN quantum dot photocell),  $E_1 - E_c = 0.6$  meV,  $E_v - E_b = 0.6$  meV,  $\gamma_1 = \gamma_2 = \gamma$ ,  $\tilde{\gamma}_1 = 100\gamma$ ,  $\tilde{\gamma}_2 = 10^{-2}\gamma$  and  $\tilde{\Gamma} = 0.05\gamma$ . In this example, microwave induced coherence increases the peak power by about 100% for  $\Omega \sim 100\gamma$ . Power saturation occurs at  $\Omega \sim 500\gamma$ .

Enhancement of the power can be explained as follows. Suppose a solar photon with energy resonant to either  $E_{1b} = E_1 - E_b$  or  $E_{2b} = E_2 - E_b$  transitions is absorbed and an electron is promoted from the valence state  $|b\rangle$  to the conduction states  $|1\rangle$  or  $|2\rangle$ . Then the electron may proceed to the conduction reservoir state  $|c\rangle$  and produce useful work by passing through a load and returning to state  $|b\rangle$  via  $|v\rangle$ . On the other hand the electron may fall back to  $|b\rangle$  via stimulated or spontaneous emission of a solar photon of energy  $E_{1b}$  or  $E_{2b}$ . To minimize this radiative recombination process we use external

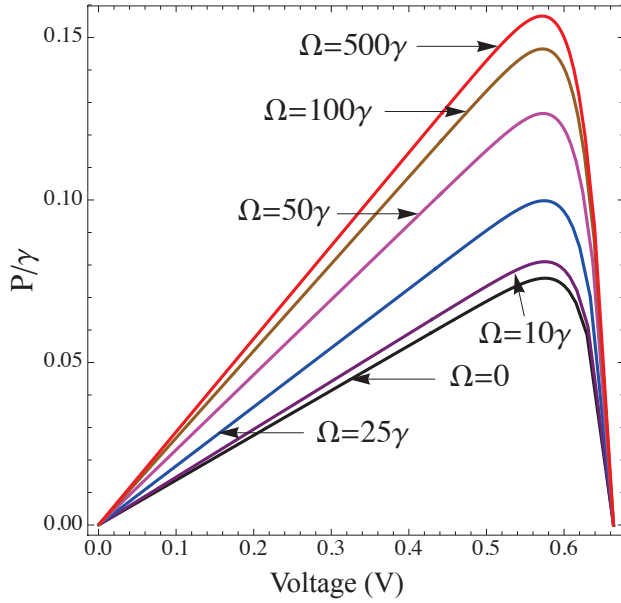


FIG. 2. (Color online) Power as a function of voltage for PV cell with upper level doublet driven by microwave for different values of the microwave field Rabi frequency  $\Omega$ .

microwave source which creates coherence that yields faster transfer of electrons into the conduction state  $c$ .

On the other hand one might argue that an incoherent external drive can also enhance photocurrent without inducing coherence. For example, if decay rates  $\tilde{\gamma}_1$  and  $\tilde{\gamma}_2$  are different by orders of magnitude, e.g.  $\tilde{\gamma}_1 \gg \tilde{\gamma}_2$ , the strong driving field transfers population from  $|2\rangle$  to  $|1\rangle$  very effectively, which is then transferred to the level  $|c\rangle$  at the larger rate  $\tilde{\gamma}_1$ , thus increasing the cell current.

In order to reveal the effect of coherence on the photocell power we study influence of decoherence  $\tau_2$ . Figs. 3, 4 and 5 show cell power, current and coherence  $\rho_{12}$  as a function of voltage across the load for  $\Omega = 50\gamma$  and different values of decoherence rate  $\gamma_\tau = 0, 10\tilde{\gamma}_1, 50\tilde{\gamma}_1$  and  $500\tilde{\gamma}_1$ . The other parameters are the same as in Fig. 2. The plots demonstrate that at fixed drive  $\Omega$  the photocell power and current reduce with increasing  $\gamma_\tau$  (decreasing coherence  $\rho_{12}$ ). At very large  $\gamma_\tau$  coherence vanishes (as per Fig. 5). In this limit the photocell power is reduced almost upto its value with no drive (see Fig. 3). Hence, for the chosen photocell parameters, coherence  $\rho_{12}$  is an essential ingredient in improving the cell performance because microwave drive itself practically does not change the cell power unless it induces coherence  $\rho_{12}$ .

One should note that in the present example coherence is robust against environmental decoherence  $\tau_2$ . Namely, in order to suppress  $\rho_{12}$  the decoherence rate  $\gamma_\tau$  should be much greater than the fastest spontaneous decay rate  $\tilde{\gamma}_1$ . Even if  $\gamma_\tau = 50\tilde{\gamma}_1$  the value of coherence is reduced only by a factor of two (see Fig. 5). Large phonon occupation numbers  $n_{c1}$  and  $n_{c2}$  are the reason for weak effect of  $\tau_2$ . In such a case

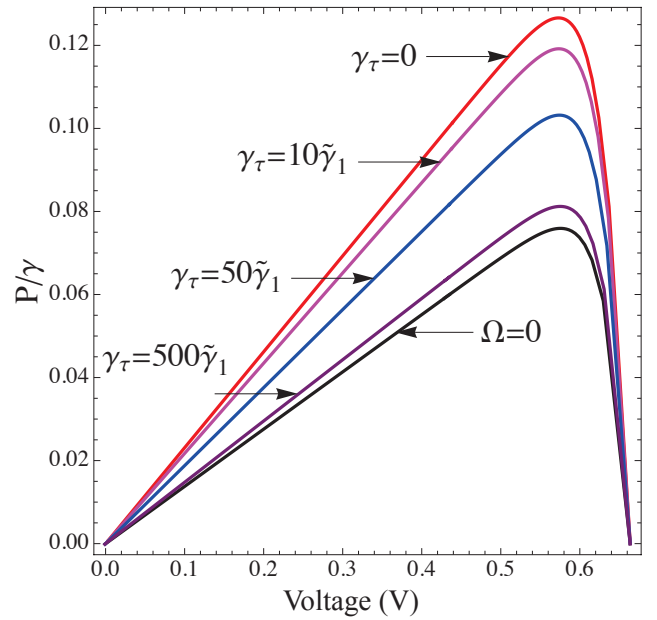


FIG. 3. (Color online) Power of a photocell of Fig. 1 as a function of voltage for different decoherence rates  $\gamma_\tau = 0, 10\tilde{\gamma}_1, 50\tilde{\gamma}_1$  and  $500\tilde{\gamma}_1$ , where  $\tilde{\gamma}_1$  is the fastest spontaneous decay rate in the system. Other parameters are indicated in the text.

decoherence due to stimulated phonon emission is the dominant decoherence channel with which  $\gamma_\tau$  should compete to suppress  $\rho_{12}$  [13].

In summary, we show that coherence induced by an external source can substantially increase photocell power. The extra power produced by the device is much larger than those acquired from the microwave source to create coherence. Physically, induced coherence results in utilization of a larger amount of solar photons by increasing solar photon absorption or quenching unwanted emission. This yields power enhancement. We demonstrate the key role of coherence in improving the cell operation by showing that suppression of coherence (e.g. due to increase in the decoherence rate  $\gamma_\tau$ ) at fixed driving field results in reduction of the output power. Utilization of quantum coherence in photocells might be a useful tool for improving their performance.

#### ACKNOWLEDGMENTS

We gratefully acknowledge support for this work by National Science Foundation Grant EEC-0540832 (MIRTHE ERC), the Office of Naval Research and Robert A. Welch Foundation (Award A-1261).

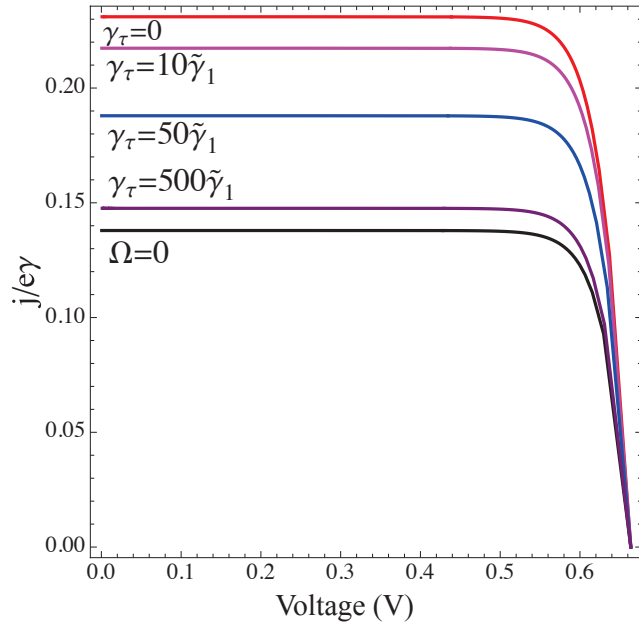


FIG. 4. (Color online) Current voltage characteristics of PV cell of Fig. 1 for the same parameters as in Fig. 3.

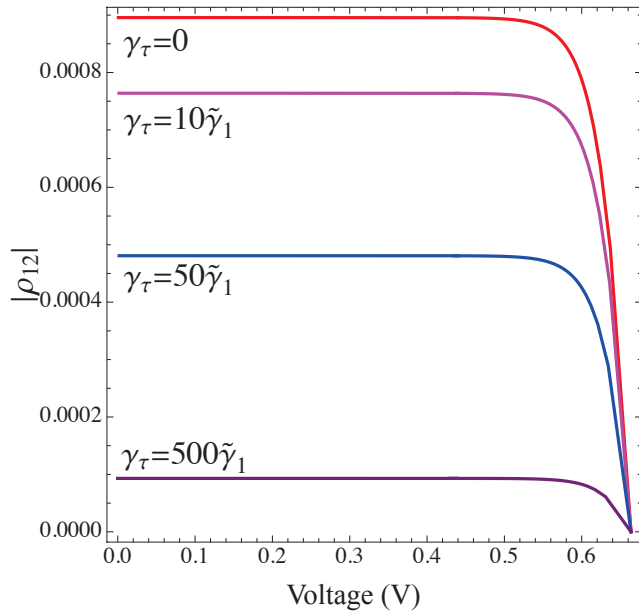


FIG. 5. (Color online) Coherence between levels 1 and 2 for PV cell of Fig. 1 for the same parameters as in Fig. 3.

- 
- [1] For a review see O. Kocharovskaya, Phys. Rep. **219**, 175 (1992); S. Harris, Phys. Today **50**, 36 (1997).
- [2] M.O. Scully and M.S. Zubairy, Quantum Optics (Cambridge University Press, Cambridge, UK, 1997).
- [3] M. Fleischhauer, A. Imamoglu and J.P. Marangos, Rev. Mod. Phys. **77**, 633 (2005).
- [4] L.V. Hau, S.E. Harris, Z. Dutton and C.H. Behroozi, Nature **397**, 549 (1999); M.M. Kash *et al.*, Phys. Rev. Lett. **82**, 5229 (1999).
- [5] W.W. Chow, H.C. Schneider and M.C. Phillips, Phys. Rev. A **68**, 053802 (2003); W.W. Chow, S. Michael and H.C. Schneider, J. Mod. Opt. **54**, 2413 (2007).
- [6] A.A. Belyanin, F. Capasso, V.V. Kocharovsky, V.I. Kocharovsky and M.O. Scully, Phys. Rev. A **63**, 053803 (2001).
- [7] The quantum photon engine is treated in M. Scully, S. Zubairy, G. Agarwal, and H. Walther, Science **299**, 862 (2003). The classical photon heat engine is nicely discussed in M. H. Lee, Am. J. Phys. **69**, 874 (2001).
- [8] H.E.D. Scovil and E.O. Schulz-DuBois, Phys. Rev. Lett. **2**, 262-263 (1959).
- [9] W. Shockley and H.J. Queisser, J. Appl. Phys. **32**, 510-519 (1961).
- [10] S. Harris, Phys. Rev. Lett. **62**, 1033 (1989).
- [11] M. Scully, Phys. Rev. Lett. **104**, 207701 (2010).
- [12] A. Svidzinsky, K. Dorfman and M. O. Scully, to be published in Phys. Rev. A (2011).
- [13] A. Svidzinsky, K. Dorfman and M. O. Scully, to be published in New Journal of Physics (2011).
- [14] U. Fano, Phys. Rev. **124**, 1866 (1961).
- [15] K.E. Dorfman, P.K. Jha and S. Das, arXiv:1108.1567v1, to be published in Phys. Rev. A (2011).
- [16] Another interesting connection can be made with the quantum efficiency of the laser without inversion as discussed in M. Scully, Phys. Rev. Lett. **106**, 049801 (2011); arXiv:1012.5321v2 [quant-ph].
- [17] M.O. Scully, K.R. Chapin, K.E. Dorfman, M.B. Kim, and A.A. Svidzinsky, PNAS **108**, 15097 (2011).